

ASSESSMENT OF AN OBLIQUE MOVING DEFORMABLE BARRIER TEST PROCEDURE

James Saunders

Dan Parent

National Highway Traffic Safety Administration (NHTSA)
USA

Paper Number: 13-0402

ABSTRACT

In September 2009 the National Highway Traffic Safety Administration (NHTSA) published a report that investigated the incidence of fatalities to belted non-ejected occupants in frontal crashes involving late-model vehicles. The report concluded that after exceedingly severe crashes, the largest number of fatalities occurred in crashes involving poor structural engagement between the vehicle and its collision partner, such as corner impacts, oblique crashes, or impacts with narrow objects.

In response to these findings, NHTSA began researching a test procedure intended to mitigate the risk of injuries and fatalities related to motor vehicle crashes involving poor structural engagement. This research demonstrated that an offset impact between a “research” moving deformable barrier (RMDB) and a stationary vehicle at a 15 degree angle can reproduce vehicle crush, occupant kinematics, and risk of injury seen in vehicle-to-vehicle crashes. It was also demonstrated that injury risk related to poor structural engagement has not been entirely mitigated in the current fleet, as newly-designed vehicles are still prone to large intrusions and potential injuries to the head, chest, knee/thigh/hip, and lower extremity.

The current study adds additional oblique RMDB-to-vehicle crash tests with high sales volumes vehicles in order to capture a larger portion of the current and future fleet for further analysis. These additional tests bolster the utility of the existing database of oblique RMDB-to-vehicle crash tests with a THOR 50th percentile male occupant in the driver’s seat.

INTRODUCTION

Saunders et al, 2012 [1] performed paired vehicle test in both “Small Overlap Impact” (SOI) and “Offset

Oblique” (Oblique) test procedures with vehicles that were redesigned or introduced in 2010 and 2011. Most of these vehicles received the highest ratings in current US consumer rating systems. Saunders et al, 2012 [1] demonstrated that even though these vehicles had good ratings in consumer information crash tests and were newly designed, there still exists potential for vehicle design improvements that could mitigate real-world injuries and fatalities in both of these crash types. When comparing the average injury assessment values (IAVs) for each body region in each of the two procedures, similar trends appeared in both the SOI and Oblique test modes, which mirrored the real-world data, including the risk of knee-thigh-hip, lower extremity, head, and chest injuries. There were, however, some differences in IAVs between the SOI and the Oblique modes; head and chest IAVs were slightly higher in Oblique, while knee-thigh-hip IAVs were higher in SOI. Rudd et al. 2011 [4] also found similar findings when they reviewed Oblique and SOI vehicle crashes included in the Crash Injury Research and Engineering Network (CIREN) and National Automotive Sampling System Crashworthiness Data System (NASS-CDS) databases.

Saunders et al, 2013 [2] demonstrated that the repeatability of the two test procedures were similar to existing vehicle tests in the full frontal and offset deformable barrier crash test conditions.

To help support NHTSA’s decision on its small overlap/oblique program, this paper adds addition high sales volume vehicles to the previous study in order to capture the safety performance of a larger portion of the current and future fleet. In addition to the previous left-side Oblique test configuration, this paper presents Oblique impacts to the right side of the vehicle and evaluates the kinematics of an

occupant positioned on the non-struck side of the vehicle.

METHODOLOGY

Oblique Crash Testing

Figure 1 shows the left side impact (LSI) Oblique test procedure setup. In this setup, the RMDB impacts the target vehicle at 90 kph (56 mph) and the stationary vehicle is positioned such that the angle between the RMDB and the vehicle is 15 degrees and the overlap is 35 percent on the driver side of the vehicle.

The vehicle was instrumented with a rear accelerometer to record the X and Y accelerations of the vehicle. Between test series some of the procedures for measuring intrusions were modified, therefore the following list gives the general locations of the intrusions measured for each test.

1. A 4 by 5 matrix of points on the toepan/floorboard (Figure 2). The location with the maximum X intrusion is used for analysis in this paper.
2. Left and right instrument panel (Figure 2)
3. Steering wheel (Figure 2),
4. Bottom A-pillar (B A-pillar) (Figure 3)
5. Rocker panel (Figure 3)

Table 1 shows the list of vehicles tested in LSIs and Table 2 shows the list of vehicles that were tested in right side impacts (RSI). Throughout this paper, the LSI conditions are referenced by the vehicle name itself, and the RSI conditions are referenced by the vehicle name followed by an “R” to indicate the right-side impact.

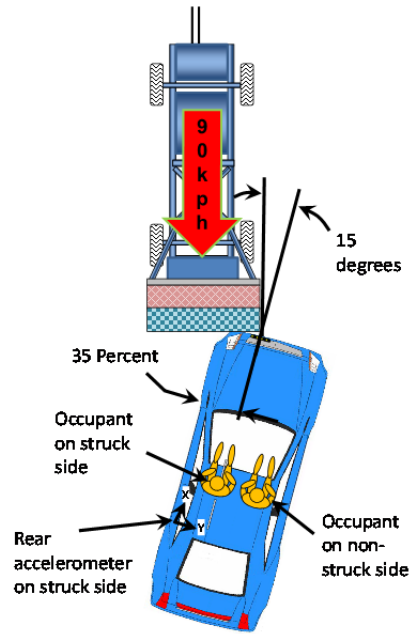


Figure 1: Test setup for LSI

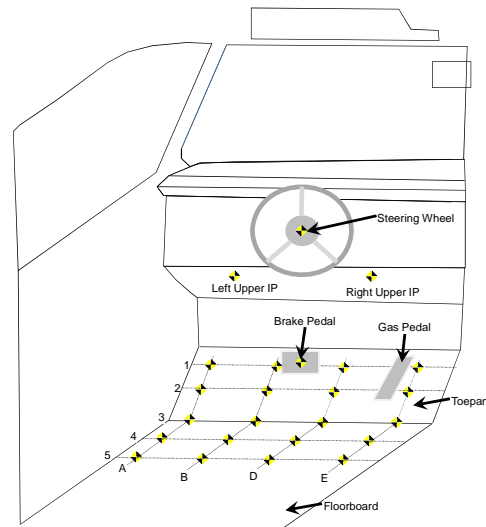


Figure 2: Interior intrusion measurements



Figure 3: Location of B A-pillar and rocker panel intrusion points

Table 1: LSI matrix and naming convention of each vehicle

| NHTSA TEST NUMBER | MAKE | MODEL | YEAR | TEST WEIGHT (KG) |
|-------------------|-----------|-----------|------|------------------|
| 7458 | Smart | Fortwo | 2011 | 1034 |
| 7441 | Toyota | Yaris | 2011 | 1331 |
| 7428 | Ford | Fiesta | 2011 | 1371 |
| 8084* | Nissan | Versa | 2013 | 1451 |
| 8089* | Hyundai | Elantra | 2013 | 1590 |
| 7431 | Chevrolet | Cruze | 2011 | 1662 |
| 8088* | Toyota | Camry | 2012 | 1759 |
| 7467 | Buick | LaCrosse | 2011 | 1944 |
| 8087* | Ford | Taurus | 2013 | 2123 |
| 8097* | Honda | Odyssey | 2012 | 2210 |
| 8096* | Honda | CRV | 2012 | 1757 |
| 7476 | Ford | Explorer | 2011 | 2363 |
| 7457 | Dodge | RAM1500 | 2011 | 2611 |
| 8099* | Chevrolet | Silverado | 2012 | 2624 |

* THOR positioned in both driver and right front seating position

Table 2: RSI matrix and naming convention of each vehicle

| NHTSA TEST NUMBER | MAKE | MODEL | NAME | TEST WEIGHT (KG) |
|-------------------|--------|--------|------|------------------|
| 8086* | Nissan | VersaR | 2013 | 1438 |
| 8085* | Toyota | CamryR | 2012 | 1752 |

* THOR positioned in both driver and right front seating position

Occupant Response Assessment

Previous Oblique RMDB crash tests included an anthropomorphic test device (ATD) seated in the driver (near-side) position. This ATD was a 50th percentile male Test Device for Human Occupant Restraint (THOR) which met the specifications of the Mod Kit [5]. For the most recent 7 of the LSI tests included in this study, a second THOR was seated in the right front passenger seat (far-side) (Table 1). The far-side THOR met the specifications of the Mod Kit, with the addition of a shoulder assembly intended to improve anthropometry and biomechanical response of the shoulder-torso complex. This shoulder assembly, known as the “SD-3,” is a derivation of the Chalmers shoulder [6] which was further developed through the European Union’s

THORAX project [7]. Since only one SD-3 shoulder assembly was available at the time of these tests, it was installed on the far-side THOR to investigate the interaction with the shoulder belt when the occupant is moving laterally away from the belt, while minimizing the risk of damage due to direct contact with the door which would be more likely on the near-side.

For the RSI tests, the ATDs positions were reversed such that the THOR with the SD-3 shoulder was in the driver (now far-side) position and the THOR with the standard shoulder was in the passenger (now near-side) position. In both the LSI and the RSI conditions, each ATD was positioned according to the Federal Motor Vehicle Safety Standard (FMVSS) No. 208 seating procedure.



Figure 4. Position of two THOR ATDs in the driver and front passenger position.

RESULTS

Vehicle Response

In general, the total velocity change (delta-V (DV)) in the X-direction decreases as the weight of the vehicle increases for both LSI and RSI (Figure 5). One exception to this general trend occurs with the Versa, where the RSI condition fits the general trend but the LSI condition shows a lower-than-predicted X-direction DV and a higher-than-predicted Y-direction DV. There is no general trend in Y-direction DV for either LSI or RSI.

Except for the ForTwo and the Versa, the toepan intrusion in the X-direction was between 100 mm and 150 mm (Figure 6). The maximum IP intrusion decreased as weight increased, except for the Taurus. The A-pillar intrusions were all below 50 mm, except for the ForTwo, the Fiesta, and the Versa. Only the ForTwo had a Rocker Panel intrusion higher than 50

mm. Toeplan intrusions seemed consistent for all vehicles, while the IP intrusion tended to be higher for the lightest vehicles. All steering wheel (SW) intrusion in the X-direction were below 60 mm except for the ForTwo, the Versa, and the Ram1500 (Figure 7). The Yaris, the Versa, the Cruze, and the Camry SW intrusions in the Z-direction were higher than 50 mm.

Figure 8 shows the X-direction intrusions for VersaR and CamryR. VersaR had over 200 mm intrusion for B A-pillar and Rocker Panel.

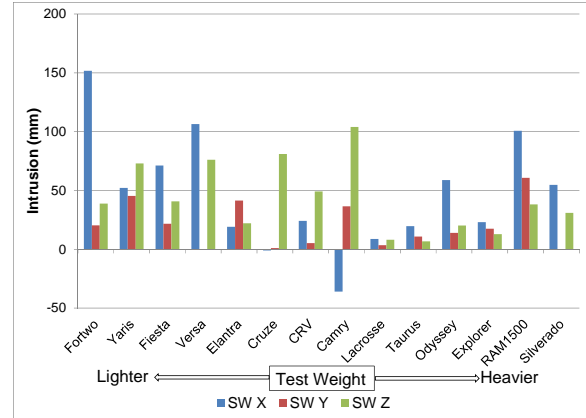


Figure 7: SW intrusions for LSI

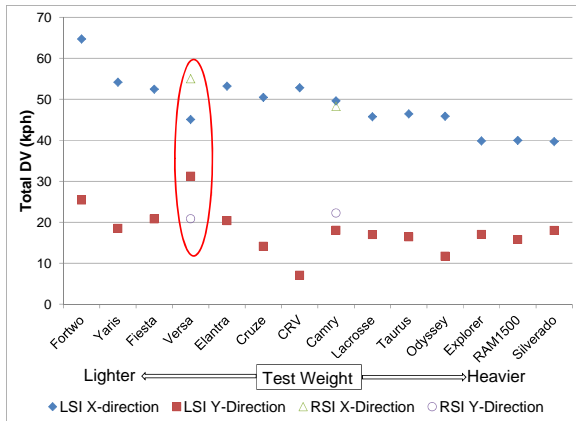


Figure 5: Total DV for LSI and RSI

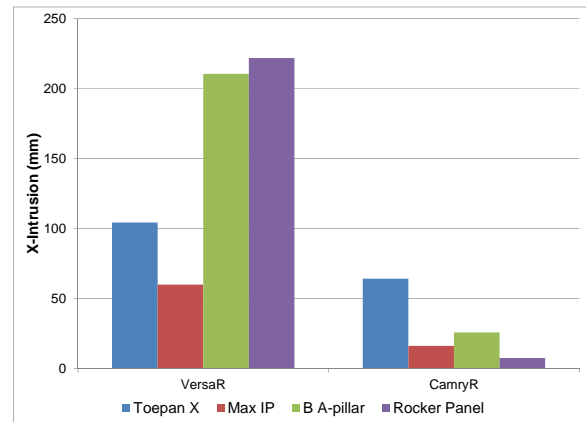


Figure 8: Intrusions for RSI

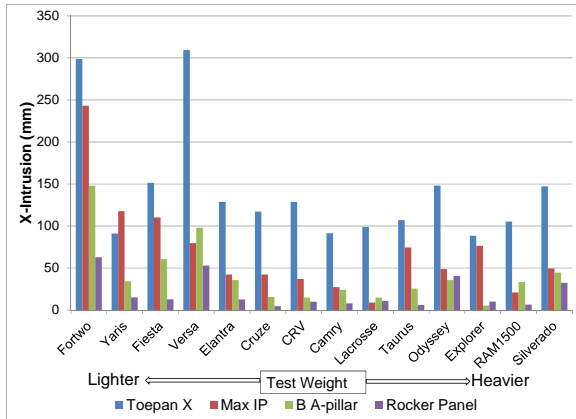


Figure 6: Intrusions for LSI

Occupant Response

Restraint Deployment

In all nine vehicle crash tests carried out, the occupant restraint systems deployed frontal air bags and safety belt pretensioners for both the driver and the right front passenger. In all but one case (LSI condition for the Taurus), a side curtain air bag was deployed on the near-side impact location. Note that the side curtain air bag on the far-side impact location was disabled to allow improved high-speed video visibility, since the principal direction of force would direct the far-side occupant away from this curtain air bag.

Frontal air bag deployment time varied across vehicles, but deployed no later than 28 milliseconds after barrier contact with the bumper of the target vehicle. Safety belt pretensioners triggered before or at the same time as the frontal air bag deployment, no

later than 20 milliseconds after impact, and triggered at the same time for both the driver and right front passenger. The side curtain air bags generally deployed later than the frontal air bags, except for the Camry and the Silverado, which deployed both frontal and side curtain air bags simultaneously. Restraint deployment times and head contact locations are summarized in the Appendix (Table 3).

Lap belt loads varied with no apparent relationship to vehicle mass or DV in both the near-side and far-side occupant locations. For the near-side (Figure 9), the lightest vehicle had the lowest peak lap belt load while the second-lightest vehicle had the highest peak lap belt load, while other tests were clustered around the mean ($\mu = 3590$ N, $\sigma = 1860$ N). For the far-side (Figure 10), there was a large range and dispersion of peak lap belt forces ($\mu = 5870$ N, $\sigma = 1850$ N).

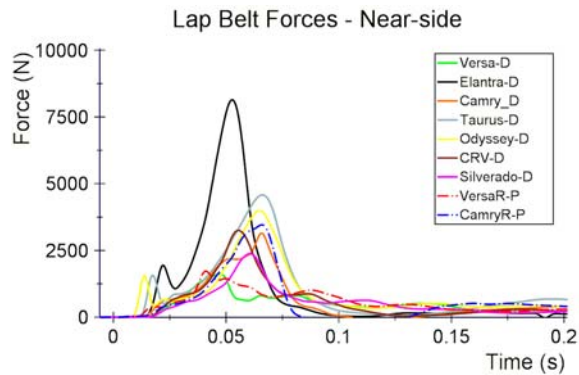


Figure 9. Lap belt forces in the near-side occupant location.

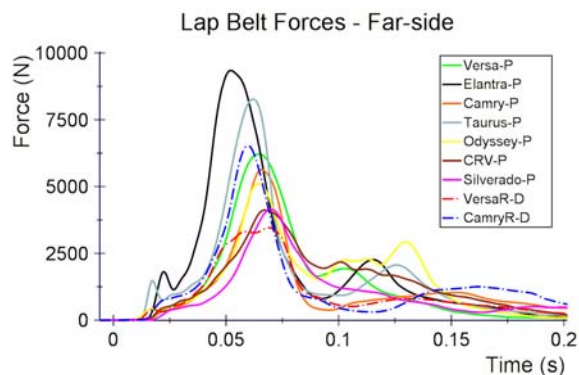


Figure 10. Lap belt forces in the far-side occupant location.

Peak shoulder belt loads were more consistent for both the near-side (Figure 11; $\mu = 4160$ N, $\sigma = 730$

N) and the far-side (Figure 12; $\mu = 4030$ N, $\sigma = 920$ N) occupant locations, though the shoulder belt load cell for the near-side occupant failed in two tests. In the far-side shoulder belt force time-histories, there are several abrupt drops in the force shortly after the time of peak load, the most obvious occurring in the Taurus between 65 and 70 milliseconds and in the Versa between 50 and 55 milliseconds. These times may correspond to the time that the shoulder belt loses engagement with the shoulder and slides laterally away from the torso.

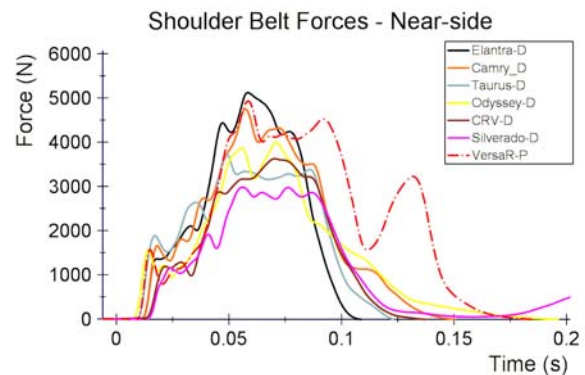


Figure 11. Shoulder belt forces in the near-side occupant location.

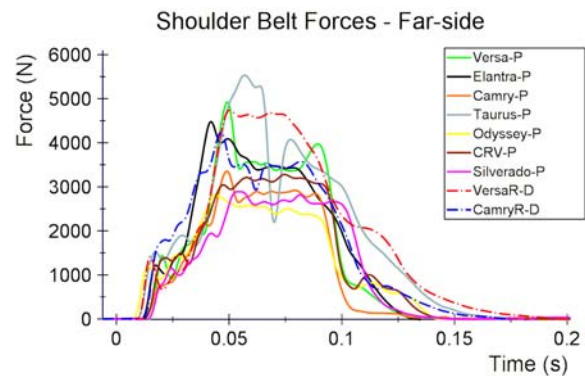


Figure 12. Shoulder belt forces in the far-side occupant location.

Near-side Occupant Kinematics

In the LSI condition, the occupant in the driver's seat begins moving directly forward with a gradually-increasing outboard translation. The head contacts the center or left-center of the frontal air bag with a laterally outboard velocity and is deflected towards the side curtain air bag. Contact with the side curtain air bag was generally minor and focused on the left side of the head, and in one condition (Silverado) the head only contacted the side curtain air bag on

rebound. The head then translates into the gap between the frontal air bag and the side curtain air bag and contacts the door panel. Though, in most cases it was a glancing blow that did not impart much acceleration on the head.

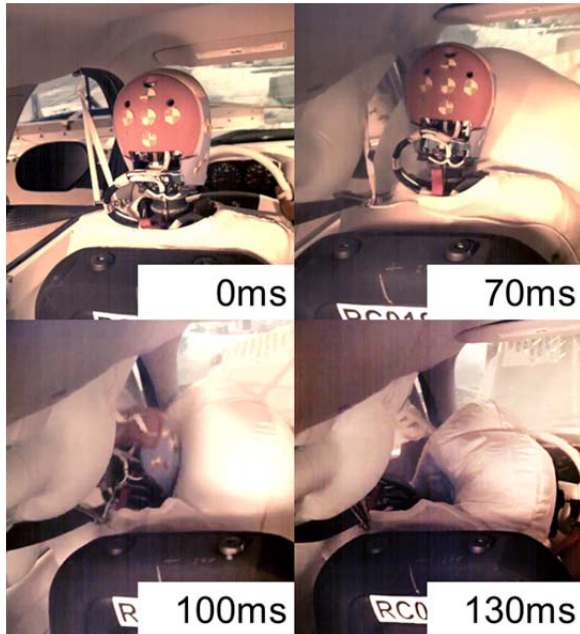


Figure 13. Near-side occupant head kinematics in the LSI Silverado test.

In the RSI condition, the occupant kinematics were essentially a mirror-image of the kinematics in the LSI condition. The occupant moved forward and to the right, the head glanced off the frontal airbag to the right and moved into the gap between the frontal and side curtain air bags. In the Versa, the occupant contacted the door frame at the window sill (Figure 14), while in the Camry, the occupant showed initial upward motion that resulted in contact with the roof (Figure 15). This initial upward motion appears to be the result of a nose-down pitch of the vehicle body during the initial interaction with the RMDB.

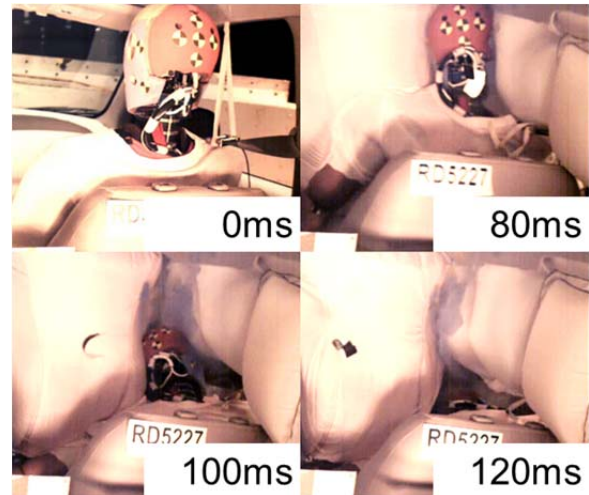


Figure 14. Head kinematics of the near-side occupant in VersaR. The head slides between the gap in the frontal and side curtain air bags and contacts the door frame.



Figure 15. Head kinematics of the near-side occupant in the CamryR test. The head initially translates upward and contacts roof at 75 ms, then continues to travel forward and outboard between frontal air bag and side curtain air bag.

Far-side Occupant Kinematics

In the LSI condition, the far-side occupant is seated in the right front passenger seat. Like the near-side occupant location, the ATD begins moving forward with an increasing left lateral trajectory. In all of the LSI vehicles, the frontal air bag is fully inflated by the time of head contact. Though, unlike the near-side location where the bag is initially closer to the occupant, the head of the far-side occupant always contacts left-of-center on the frontal air bag (Figure 16). Friction between the head and the air bag results in positive rotation of the head about its local Z-axis. In most cases the head then contacts the center IP, either through the bag or directly leaving a paint transfer. Two exceptions to this behavior were the Taurus, where the head remained in contact with the frontal air bag for the duration of the crash event, and the Silverado, where the far-side occupant translated far enough laterally to contact the steering column-mounted gear shift lever. In all of the LSI conditions, the torso of the occupant translates laterally away from the shoulder belt and the belt loses engagement with the shoulder at around 100 milliseconds after the impact.

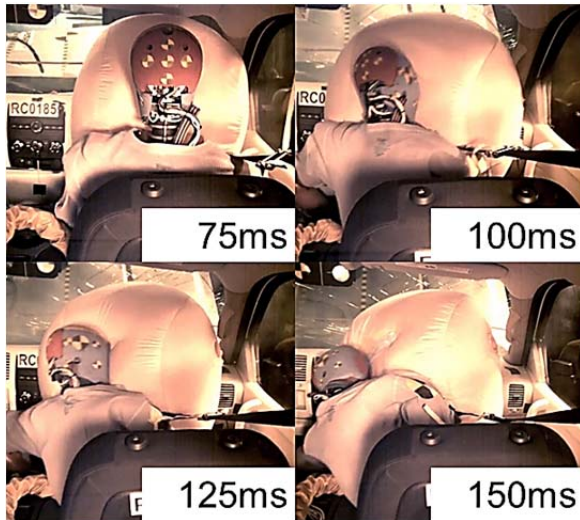


Figure 16. Typical kinematics of the far-side occupant in the LSI condition (Silverado in this case).

In the RSI condition, the kinematics were a mirror-image of the LSI condition with a few exceptions related to the differences in driver-side and passenger-side restraints. The frontal air bag on the driver side is initially closer to the occupant, so head

contact occurs with the center of the air bag before lateral translation begins. Though, similar to the far-side occupant in the LSI condition, friction between the RSI far-side occupant's head and the driver-side air bag results in head rotation away from the principle direction of force (PDOF) about its local Z-axis. Since the THOR is positioned with its hands on the steering wheel, similar to the positioning of a Hybrid III in the FMVSS No. 208 seating procedure, the arm ends up between the head and the center IP at the point of peak head excursion. For both of the RSI tests, the head of the far-side occupant contacts the right forearm which is in contact with the center IP at the point of peak excursion (Figure 17). Like the LSI condition, the torso of the far-side occupant in the RSI condition translated away from the shoulder belt, losing engagement with the shoulder at around 100 milliseconds after the impact.

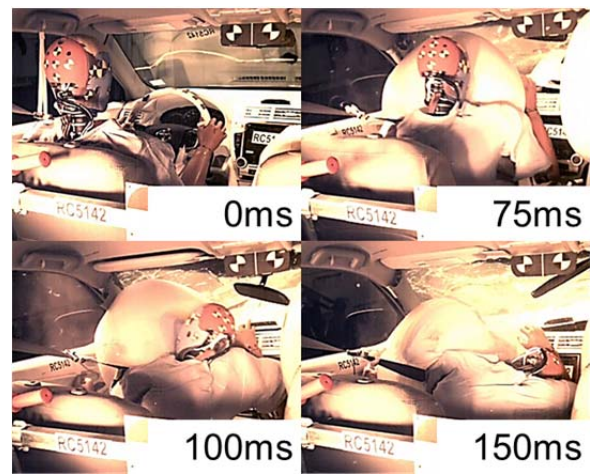


Figure 17. Typical kinematics of the far-side occupant in the RSI condition (CamryR in this case).

Occupant Injury Assessment

A set of IAV metrics were selected based on the available measurements and the existence of preliminary injury assessment reference values (IARVs) for the THOR ATD. IAVs are calculated for each test, whereas IARVs refer to tolerance values, usually tied to a given probability of a certain injury, used to assess the relative severity of the occupant response. As an overall assessment, the metrics that suggest the highest probability of injury include the kinematic brain injury criterion (BRIC),

acetabulum resultant force, tibia index, and ankle rotation. These metrics show good agreement with the field injury exposure presented by Rudd et al 2011 [4], where the body regions with the highest incidence of injury were the knee/thigh/hip, chest, lower extremity, and head. Summaries of the IAVs calculated for the near-side (Table 4) and far-side (Table 5) occupants are included in the Appendix, while this section will focus on the head, chest, knee/thigh/hip, and lower extremity. This section will describe the response of occupants in both the driver seat (near-side occupant in LSI and far-side occupant in RSI) and the right front passenger seat (far-side occupant in LSI and near-side occupant in RSI).

Head

Four out of the eighteen sets of occupant IAVs exceeded the provisional IARV for the 15 ms head injury criteria (HIC15) (Figure 18). All four of these instances coincide with the time of contact of the head to either the door panel (for near-side occupants) or the center IP (for far-side occupants). The head acceleration in the near-side impacts was equally high in the local X- and Y- directions, suggesting a 45 degree effective angle of contact with the door panel. The head acceleration in the far-side impacts was primarily oriented in the positive Y-direction, since the head in both of these cases was rotated 90 degrees to the right and the left side of the head impacted the center IP. There are no apparent trends of HIC15 with vehicle mass, LSI vs. RSI, or near-side vs. far-side.

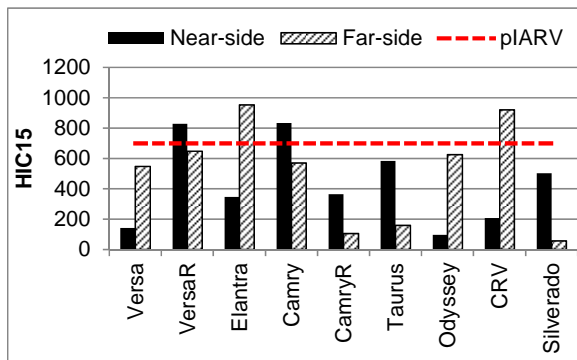


Figure 18. HIC15 head injury metric for LSI and RSI tests.

The BRIC injury assessment metric was calculated using the method and critical values described in Saunders et al, 2012 [1]. The BRIC metric considers the angular velocity and angular acceleration of the head (Eqn 1), as measured by angular rate sensors installed in the head of the THOR ATD. Five out of the nine near-side occupants exceeded the provisional IARV for BRIC of 0.89 (Figure 19), which corresponds to a 30% risk of AIS 3+ traumatic brain injury [8]. One of the highest BRIC values occurred in the Taurus for the near-side occupant, where there was not a side curtain air bag present. While there was a spike in angular acceleration upon contact with the door frame, the primary factor in exceeding the BRIC provisional IARV was the local head X- and Z-direction angular velocity imparted to the head after contact with the frontal air bag.

$$BRIC = \frac{\omega_{max}}{\omega_{cr}} + \frac{\alpha_{max}}{\alpha_{cr}} \quad (1)$$

In all nine of the far-side cases, the calculated BRIC was higher than the provisional IARV (Figure 19). In each test, head contact with the frontal air bag imparted an outboard rotational velocity on the head about its local Z-axis. Angular velocity was the driving factor in the BRIC metric, as four out of the nine far-side occupants would have exceeded the BRIC provisional IARV based on the angular velocity component alone. On the other hand, none of the near-side or far-side responses would have exceeded the BRIC provisional IARV based on the angular acceleration component alone.

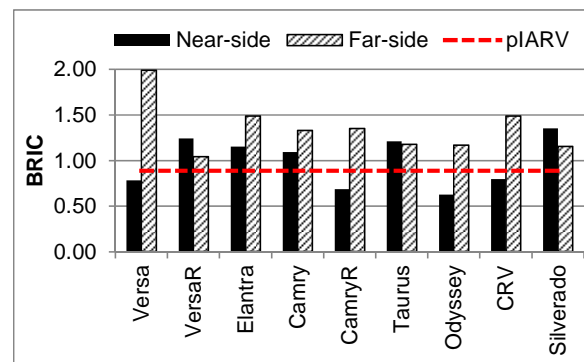


Figure 19. BRIC rotational head injury metric for LSI and RSI tests.

It is worth noting that since the head angular velocity is the driving factor in the BRIC calculation, the

timing of the HIC and BRIC IAVs are not coincident. As an example, consider the near-side (right front passenger seat) occupant in the CamryR test (Figure 20). The head linear acceleration results in a HIC₁₅ window of between 59 and 72 milliseconds. While there is an increase in head angular velocity in this same time window, the peak angular velocity does not occur until 130 milliseconds.

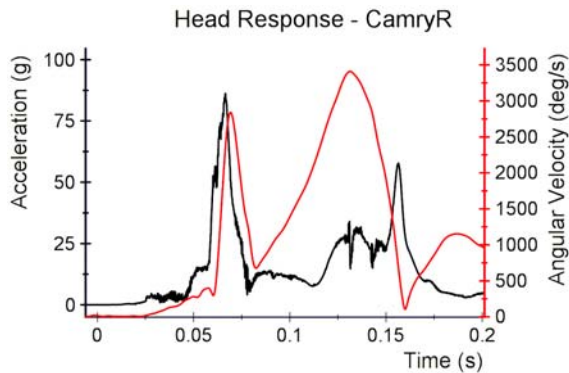


Figure 20. Near-side head resultant linear acceleration (black) and angular velocity (red) in CamryR.

Chest

Chest deflections presented in Figure 21 represent the maximum deflection at any of the four chest quadrants measured by the THOR ATD at any point in time. This deflection is calculated as the peak change in length of the vector between the attachment point of the thoracic deflection instrumentation on the anterior rib cage and the anchor point on the local spine segment. In all but one of the tests in this series (Versa LSI), chest deflection was higher for the near-side occupant than for the far-side occupant.

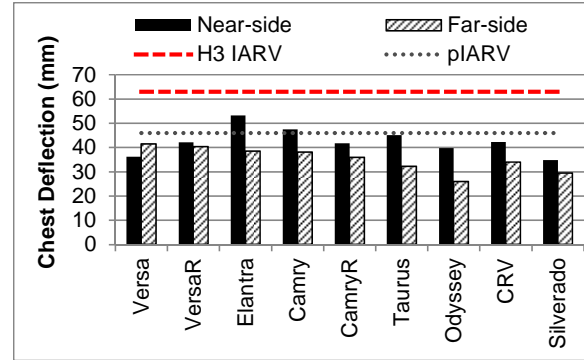


Figure 21. Peak chest deflection for LSI and RSI tests.

The relationship between injury risk and chest deflection as measured by the THOR ATD has not yet been developed. Figure 21 shows the existing IARV for the Hybrid III 50th percentile male (63 millimeters) as well as a provisional IARV (46 millimeters). This provisional THOR IARV was selected based on a limited series of PMHS tests which measured the three-dimensional rib deflections at the same locations as the THOR ATD. In these PMHS tests, the average deflection of the lower measurement location on the same side as the belt (which was the peak deflection location in a majority of the near-side occupants in the LSI and RSI tests) was 45.8 millimeters, which resulted in at least 2 and as many as 27 rib fractures [9]. Research is currently underway to further develop the injury risk functions and associated IARVs for rib deflection measured by the THOR ATD.

Knee/thigh/hip

While the loads measured by the distal femur and acetabulum are intrinsically related due to the shared load path, some divergent trends were observed. While none of the tests in this series exceeded the provisional femur compressive force IARV (Figure 23), eight of the tests exceed the provisional IARV for resultant acetabulum load (Figure 22). Femur loads were highest for the near-side occupant in all but one of the vehicles, while acetabulum loads were higher for the near-side occupant in only five of the nine vehicles. The highest acetabulum loads were recorded in the lightest (Versa) and the two heaviest (CRV, Silverado) vehicles.

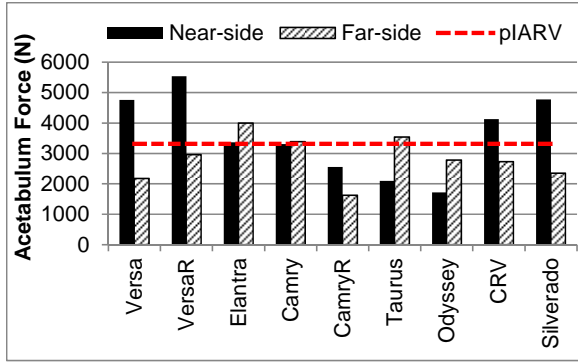


Figure 22. Peak acetabulum force in LSI and RSI tests.

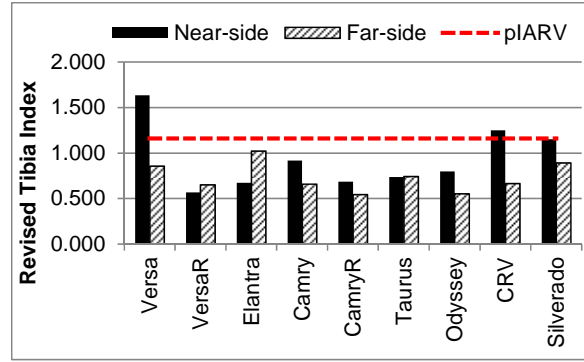


Figure 24. Maximum Revised Tibia Index in LSI and RSI tests.

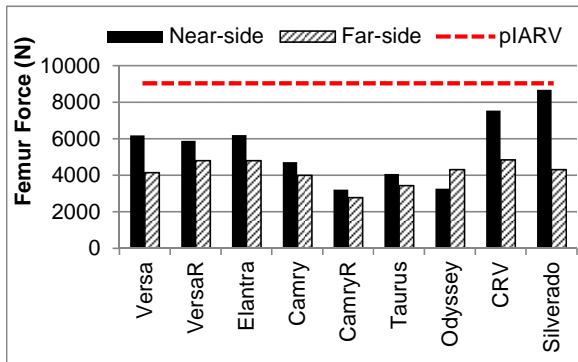


Figure 23. Peak femur compressive force in LSI and RSI tests.

Lower Extremity

The near-side occupant generally recorded a higher risk of lower extremity injury, quantified here using the Revised Tibia Index (Figure 24). This result was expected since intrusion into the occupant compartment is more likely on the near-side than the far-side. While this effect was exaggerated in the lightest (Versa) and heaviest (CRV, Silverado), there wasn't a consistent difference in the remainder of the vehicles. In one case (Elantra) the Tibia Index was noticeably higher in the far-side occupant location, though both values were below the provisional IARV.

DISCUSSION

Vehicle Response

It is normally assumed the vehicle response would be similar when impacted on the left or right of the vehicle. This appeared to be true for both intrusions and DVs for Camry and CamryR, but there were some apparent differences between the Versa and VersaR, conditions. In the LSI condition for the Versa, the toepan had the highest intrusion in the X-direction with over 300 millimeters of intrusion. VersaR showed the highest X-direction intrusion at the Bottom A-pillar and rocker panel, while the toepan intrusion was only 100 millimeters (Figure 25). Versa and VersaR DVs in the X- and Y-directions differed by around 10 kph (Figure 26).

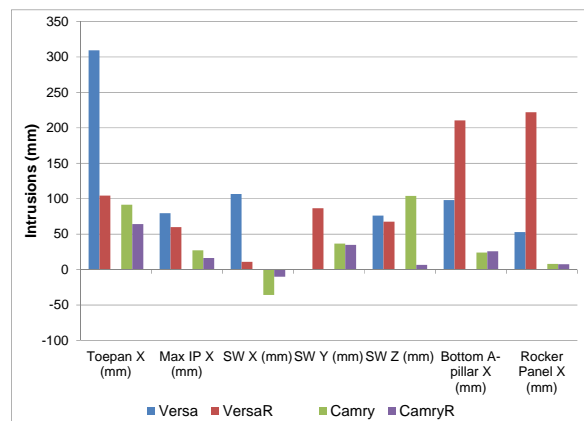


Figure 25. Comparison of intrusions between LSI and RSI

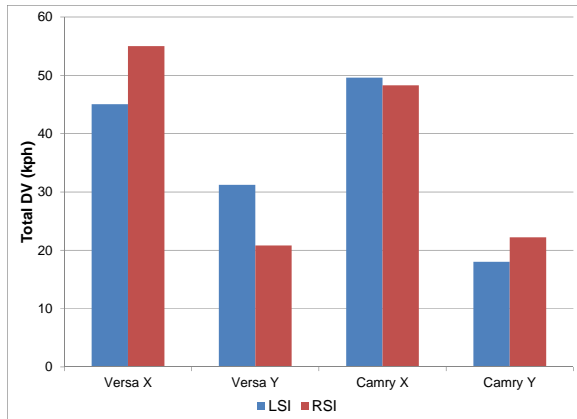


Figure 26: Comparison of Total DV between LSI and RSI

After the crash tests, it was noticed that the RSI condition had different frontal crush patterns than the LSI condition. In the LSI condition of the Versa, the frame and bumper were pushed inwards (Figure 27), whereas for VersaR the bumper was pushed straight back (Figure 28). Also, the separation of the wheel well and rocker panel may have caused the differences in the crush between Versa and VersaR (Figure 29).

Saunders et al, 2013 [2] showed that the max difference from three repeat test of a Chevrolet Cruze in the toepan and Rocker Panel was 14mm and 59 mm, respectively. Saunders also showed the max difference in DV was 2.4 kph. Even though, some of the differences in the LSI versus RSI may be explained by test variability, the difference is most likely due to asymmetric loading of the vehicle.



Figure 27: Deformation in a LSI of the Versa



Figure 28: Deformation in a RSI of the Versa

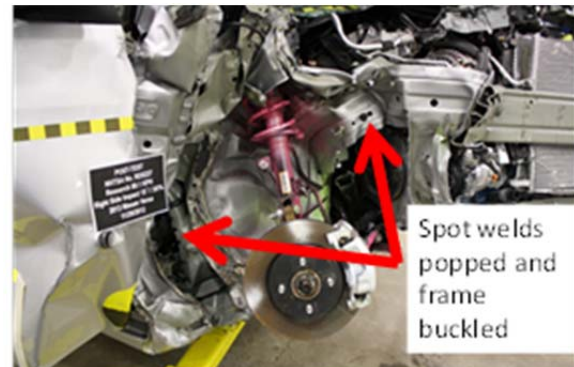


Figure 29: Buckling of the frame and separation of the wheel well and rocker panel

Occupant Response

The addition of both a right-side impact and a far-side occupant added two layers of complexity to the existing data in the Oblique RMDB crash test condition. Theoretically, the left-side impact and the right-side impact should be similar on the vehicle level, although the responses were not identical (see Figure 25 and Figure 26). Some components of the occupant response should be similar, including the acceleration pulse and interaction with the assumedly-symmetric belts and side curtain air bags, though the lack of symmetry in the frontal air bag could drive occupant response differences.

The two vehicle tests that were run in both the RSI and the LSI condition were the Versa and the Camry. In the Versa comparison, there was more engagement of the near-side occupant's head with the frontal air bag in the LSI condition, since the occupant was in the driver location and the frontal air bag was closer to the occupant initially. In contrast, the passenger's

head contacts the far outboard edge of the frontal passenger air bag in the RSI condition, which does not dissipate as much energy as the driver-side frontal air bag. The passenger's head continues to traverse forward and outboard at a higher relative velocity, resulting in a higher acceleration at the point of impact with the door panel (Figure 30).

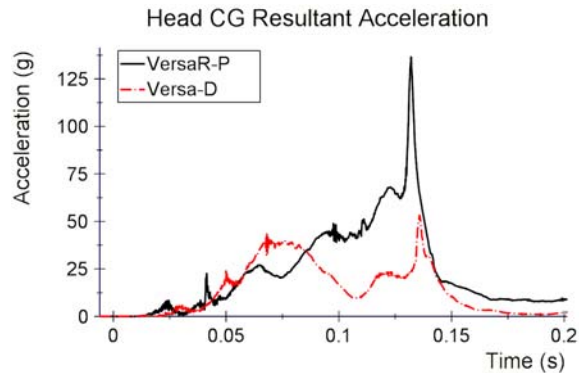


Figure 30. Near-side occupant head response in the Versa, comparing the RSI condition (black) to the LSI condition (red dash-dot).

In the Camry comparison, the occupant kinematics at the onset of the crash were noticeably different between the LSI and RSI modes. In the RSI mode, the front passenger seat appears to move upward relative to the vehicle floor, which allows upward motion of the occupant. The head contacts the roof (Figure 15), which imparts a large magnitude of acceleration early in the event (Figure 31). In the LSI mode, the same motion of the seat relative to the floor is apparent, but not at the same magnitude as in the RSI case. The driver's head does not impact the roof, but instead impacts the door frame at a higher velocity, resulting in a high acceleration peak later in the event (Figure 31).

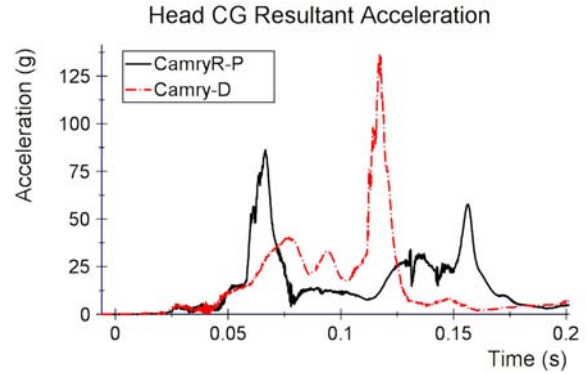


Figure 31. Near-side occupant head response in the Camry, comparing the RSI condition (black) to the LSI condition (red dash-dot).

Similar differences in head kinematics also occurred in the far-side occupant location due to the local interaction with frontal air bags of different sizes and shapes. The difference in head kinematics resulted in large discrepancies in the HIC15 and BRIC IAVs between the LSI and RSI conditions for both vehicle pairs (Figure 18, Figure 19). IAVs for other body regions, however, were relatively similar between the LSI and RSI for both the near- and far-side occupants. One other exception to this is the Tibia Index (Figure 24), where the Versa LSI near-side occupant exceeded the provisional IARV while the VersaR near-side occupant registered the lowest Tibia Index of all near-side tests.

Comparing near-side to far-side occupants, the biggest differences in the response were seen in the head region, specifically the angular rotation of the head. Interaction of the head of the far-side occupant with the frontal air bag resulted in large Z-axis rotations that were not present in most of the near-side occupant responses, with the exception of the Taurus, in which the side curtain air bag did not deploy, or the Silverado, where there was no head contact with the side curtain air bag. These cases resulted in the highest BRIC value.

The kinematics of the far-side occupant response were in part dictated by the interaction with the shoulder belt. The THOR ATD in the far-side location for each of these tests was equipped with the SD-3 shoulder, which was designed to improve occupant interaction with the shoulder belt in oblique crashes [6]. In both the LSI and RSI condition, the

far-side occupant lost engagement between the shoulder and the shoulder belt in all tests where the onboard video was available (note that the on-board high-speed video mount failed in the VersaR test, so it is not clear if and when the shoulder lost contact with the shoulder belt).

CONCLUSIONS

In general, this new set of testing of high sales volume vehicles tested in the Oblique condition showed the following:

- The near-side occupant in Oblique RMDB crash tests demonstrated similar trends and injury assessment values to the previously-evaluated Oblique tests.
- All nine of the far-side occupants measured BRIC IAVs in excess of the provisional IARV, primarily due to high angular velocities imparted by interaction with the frontal air bag and subsequent impact to the center instrument panel.
- RSI and LSI modes resulted in varied occupant kinematics due to differences in the interaction with the driver-side or passenger-side frontal air bag.
- Among the tests were two sets of LSI and RSI for the same vehicle models and the vehicle response, crush and DV were different for a LSI when compared to a RSI for the Versa, but similar for the camry vehicle tested on both sides. It should be noted that there is not enough data to conclude that the LSI and RSI vehicle responses are the same or different.

REFERENCES

1. Saunders, J., Craig, M. and Parent, D., "Moving Deformable Barrier Test Procedure for Evaluating Small Overlap/Oblique Crashes," SAE World Congress, paper no. 2012-01-0577, 2012
2. Saunders, J. and Parent, D., " Repeatability of a Small Overlap and an Oblique Moving Deformable Barrier Test Procedure," SAE World Congress, paper no. 2013-01-0762, 2013
3. Halloway, D.E., Saunders, J., Yoganandan, N. and Pintar, F. (2011) "An operational definition of small overlap impact for published NASS data." SAE World Congress, paper no. 2011-01-0543.
4. Rudd, R., Scarboro, M., Saunders, J., "Injury Analysis of Real-World Small Overlap and Oblique Frontal Crashes," 22nd ESV Conference, Paper No. 11-0384, 2011
5. Ridella, S., Parent, D., "Modifications to Improve the Durability, Usability, and Biofidelity of the THOR-NT Dummy," 22nd ESV Conference, Paper No. 11-0312, 2011.
6. Törnvall, Fredrik. A New Shoulder for the THOR Dummy Intended for Oblique Collisions. Chalmers University of Technology, 2008.
7. Lemmen, P., Been, B., Carroll, J., Hynd, D., Davidsson, J., Song, E., Lecuyer, E., "Development of an advanced frontal dummy thorax demonstrator," Proceedings of the 2012 IRCOBI Conference, 2012.
8. Takhounts, E.G., Hasija, V., Ridella, S.A., Rowson, S., Duma, S., "Kinematic Rotational Brain Injury Criterion (BRIC)," 22nd ESV Conference, Paper No. 11-0263, 2011.
9. Shaw, G., Parent, D., Purtsezov, S., Lessley, D., Crandall, J., Kent, R., Guillemot, H., Ridella, S.A., Takhounts, E., Martin, P., "Impact Response of Restrained PMHS in Frontal Sled Tests: Skeletal Deformation Patterns Under Seat Belt Loading," Stapp Car Crash Journal, 53: 1-48, November 2009.

Table 3. Head contact locations and restraint deployment timing.

| Mode | Vehicle | Contact Location (Evidence) | Frontal Air Bag Deployment | Side Curtain Air Bag Deployment | HIC15 | Pretensioner Trigger Time |
|------------------------------|------------|---|-------------------------------|------------------------------------|------------|---|
| Left Front Driver | | | | | | |
| LSI Oblique | Versa | AB (V, PT), SAB (V, PT), DP (V) | AD (18) | AD (46) | 142 | 18 |
| | Elantra | AB (V, PT), SAB (V, PT), DP (V) | AD (16) | AD (36) | 346 | 16 |
| | Camry | AB (V, PT), SAB (V, PT), DP (V, PT) | AD (26) | AD (26) | 835 | 16 |
| | Taurus | AB (V, PT), DP (V, PT) | AD (24) | AN | 584 | 14 |
| | Odyssey | AB (V, PT), SAB (V, PT) | AD (12) | AD (40) | 96 | 12 |
| | CRV | AB (V, PT), SAB (V, PT) | AD (26) | AD (44) | 207 | 18 |
| | Silverado | AB (V, PT), DP (V) | AD (20) | AD (20) | 502 | 20 |
| RSI Oblique | VersaR | AB (V, PT), IP/arm (V, PT) | AD (14) | | 647 | 14 |
| | CamryR | AB (V, PT), IP/arm (V, PT) | AD (28) | | 105 | 18 |
| Right Front Passenger | | | | | | |
| LSI Oblique | Versa | AB (V, PT), IP (V, PT) | AD (18) | | 546 | 18 |
| | Elantra | AB (V, PT), IP (V, PT) | AD (16) | | 953 | 16 |
| | Camry | AB (V, PT), IP (V, PT) | AD (26) | | 569 | 16 |
| | Taurus | AB (V, PT), IP (V) | AD (24) | | 157 | 14 |
| | Odyssey | AB (V, PT), IP (V, PT) | AD (12) | | 624 | 12 |
| | CRV | AB (V, PT), IP (V, PT) | AD (18) | | 920 | 18 |
| | Silverado | AB (V, PT), column-mount gear shift (V, PT) | AD (24) | | 56 | 20 |
| RSI Oblique | VersaR | AB (V, PT), SAB (V, PT), DP (V, PT) | AD (14) | AD (36) | 828 | 14 |
| | CamryR | AB (V, PT), SAB (V, PT), RR (V, PT) | AD (28) | AD (28) | 364 | 18 |
| | AB | Air Bag | AD () | | | Available and Deployed (time deployed in ms) |
| | SAB | Side Curtain Air Bag | | | | |
| | RR | Roof Rail | AN | | | Available and Not Deployed |
| | IP | Instrument Panel | N | | | Not Available |
| | DP | Door Panel | | | | |
| | V | Video | | | | |
| | PT | Paint Transfer | | | | |

Table 4. Summary of IAVs for near-side occupants in LSI and RSI Oblique crash tests

| Body Region | Metric | Location | Units | Ref. | Versa [8084] | VersaR [8086] | Elantra [8089] | Camry [8088] | CamryR [8085] | Taurus [8087] | Odyssey [8097] | CRV [8096] | Silverado [8099] |
|-------------|---------------|----------|-------|-------|-----------------|------------------|-------------------|-----------------|------------------|------------------|-------------------|---------------|---------------------|
| Head | HIC15 | Head CG | | 700 | 142 | 828 | 346 | 835 | 364 | 584 | 96 | 207 | 502 |
| | HIC36 | Head CG | | 1000 | 243 | 1102 | 721 | 835 | 364 | 759 | 140 | 289 | 502 |
| | BRIC | Head CG | | 0.89 | 0.78 | 1.24 | 1.15 | 1.09 | 0.69 | 1.21 | 0.63 | 0.80 | 1.35 |
| Neck | Tension | UNLC | N | 2520 | 1828 | 2486 | 2047 | 1576 | 1216 | 2002 | 1536 | 1692 | 1376 |
| | Compression | UNLC | N | -3640 | -83 | -739 | -518 | -113 | -1583 | -721 | -134 | -87 | -450 |
| Chest | Deflection | UL | mm | 63 | 10.5 | 42.2 | 19.6 | 6.1 | 30.0 | 11.0 | 10.0 | 7.9 | 7.9 |
| | Deflection | UR | mm | 63 | 36.2 | 10.9 | 37.5 | 34.1 | 10.8 | 31.7 | 27.3 | 26.3 | 26.4 |
| | Deflection | LL | mm | 63 | 10.3 | 39.1 | 5.0 | 4.6 | 41.8 | 13.2 | 6.4 | 3.9 | 9.9 |
| | Deflection | LR | mm | 63 | 34.4 | 18.4 | 53.2 | 47.5 | 11.4 | 45.1 | 39.8 | 42.3 | 34.8 |
| | Deflection | Peak | mm | 63 | 36.2 | 42.2 | 53.2 | 47.5 | 41.8 | 45.1 | 39.8 | 42.3 | 34.8 |
| | 3ms Clip | | G | 60 | 42.7 | 44.5 | 45.8 | 34.8 | 41.9 | 47.8 | 34.9 | 44.6 | 29.2 |
| Abdomen | Deflection | Peak | mm | 90 | 71.3 | 75.9 | 69.9 | 73.4 | 79.1 | 69.6 | 64.0 | 66.2 | 65.4 |
| Acetabulum | Force (Res.) | Left | N | 3316 | 4757 | 2488 | 2290 | 2951 | 1865 | 2093 | 1638 | 4132 | 3439 |
| | Force (Res.) | Right | N | 3316 | 3514 | 5540 | 3363 | 3305 | 2557 | 1948 | 1716 | 2688 | 4775 |
| Femur | Force (Axial) | Left | N | 9040 | 6185 | 3865 | 4196 | 3725 | 3090 | 2689 | 3271 | 7536 | 5970 |
| | Force (Axial) | Right | N | 9040 | 5898 | 5880 | 6202 | 4718 | 3211 | 4069 | 2898 | 5048 | 8687 |
| Tibia | Tibia Index | LU | | 1.16 | 0.830 | 0.430 | 0.503 | 0.577 | 0.637 | 0.302 | 0.734 | 0.550 | 1.151 |
| Tibia | Tibia Index | RU | | 1.16 | 1.635 | 0.526 | 0.491 | 0.779 | 0.684 | 0.641 | 0.797 | 1.134 | 0.697 |
| Tibia | Tibia Index | LL | | 1.16 | 0.779 | 0.558 | 0.604 | 0.696 | 0.427 | 0.251 | 0.791 | 0.491 | 0.783 |
| Tibia | Tibia Index | RL | | 1.16 | 0.610 | 0.567 | 0.672 | 0.917 | 0.668 | 0.736 | 0.678 | 1.248 | 0.971 |
| Tibia | Tibia Index | Max | | 1.16 | 1.635 | 0.567 | 0.672 | 0.917 | 0.684 | 0.736 | 0.797 | 1.248 | 1.151 |
| Ankle | [in/e]version | Left | deg | 35 | 22.5 | 23.7 | 30.8 | 33.7 | 27.3 | 28.5 | 13.3 | 21.2 | 42.9 |
| Ankle | [in/e]version | Right | deg | 35 | 36.5 | 41.2 | 51.8 | 40.6 | 38.7 | 33.8 | 37.5 | 35.7 | 31.4 |
| Ankle | [p/d]flexion | Left | deg | 35 | 21.4 | 21.7 | 29.5 | 36.4 | 24.1 | 36.5 | 33.7 | 37.9 | 34.7 |
| Ankle | [p/d]flexion | Right | deg | 35 | 36.6 | 43.2 | 21.3 | 18.4 | 35.6 | 27.8 | 22.5 | 35.5 | 48.2 |
| Ankle | Rotation | Max | deg | 35 | 36.6 | 43.2 | 51.8 | 40.6 | 38.7 | 36.5 | 37.5 | 37.9 | 48.2 |
| Belt | Lap Belt | Max | N | NA | 1612 | 1725 | 8143 | 3146 | 3461 | 4578 | 3997 | 3249 | 2375 |
| | Shoulder Belt | Max | N | NA | IM | 4928 | 5119 | 4749 | IM | 3733 | 3995 | 3624 | 2979 |

Table 5. Summary of IAVs for far-side occupants in LSI and RSI Oblique crash tests

| Body Region | Metric | Location | Units | Ref. | Versa [8084] | VersaR [8086] | Elantra [8089] | Camry [8088] | CamryR [8085] | Taurus [8087] | Odyssey [8097] | CRV [8096] | Silverado [8099] |
|-------------|---------------|----------|-------|-------|-----------------|------------------|-------------------|-----------------|------------------|------------------|-------------------|---------------|---------------------|
| Head | HIC15 | Head CG | | 700 | 546 | 647 | 953 | 569 | 105 | 157 | 624 | 920 | 56 |
| | HIC36 | Head CG | | 1000 | 600 | 800 | 953 | 569 | 193 | 265 | 633 | 920 | 94 |
| | BRIC | Head CG | | 0.89 | 1.99 | 1.04 | 1.49 | 1.33 | 1.35 | 1.18 | 1.17 | 1.49 | 1.15 |
| Neck | Tension | UNLC | N | 2520 | 2527 | 1M | 1465 | 1428 | 4908 | 1205 | 1977 | 2183 | 930 |
| | Compression | UNLC | N | -3640 | -145 | -23 | -752 | -1167 | -896 | -42 | -212 | -345 | -223 |
| Chest | Deflection | UL | mm | 63 | 38.5 | 16.2 | 31.4 | 33.5 | 13.2 | 32.1 | 23.9 | 33.9 | 29.4 |
| | Deflection | UR | mm | 63 | 16.8 | 40.3 | 33.3 | 38.1 | 35.8 | 27.4 | 13.7 | 17.7 | 11.9 |
| | Deflection | LL | mm | 63 | 41.4 | 5.9 | 38.5 | 30.9 | 2.5 | 32.2 | 25.9 | 27.8 | 29.0 |
| | Deflection | LR | mm | 63 | 3.0 | 30.5 | 11.1 | 11.0 | 25.3 | 11.8 | 4.9 | 6.0 | 8.7 |
| | Deflection | Peak | mm | 63 | 41.4 | 40.3 | 38.5 | 38.1 | 35.8 | 32.2 | 25.9 | 33.9 | 29.4 |
| | 3ms Clip | | G | 60 | 46.5 | 52.4 | 35.5 | 26.3 | 30.4 | 39.9 | 22.2 | 28.9 | 24.9 |
| Abdomen | Deflection | Peak | mm | 90 | 53.7 | 66.5 | 62.8 | 67.0 | 61.3 | 67.3 | 56.7 | 63.7 | 66.1 |
| Acetabulum | Force (Res.) | Left | N | 3316 | 2055 | 2956 | 3994 | 2694 | 1508 | 2624 | 1718 | 2415 | 1652 |
| | Force (Res.) | Right | N | 3316 | 2174 | 2617 | 3226 | 3379 | 1618 | 3541 | 2777 | 2724 | 2344 |
| Femur | Force (Axial) | Left | N | 9040 | 3270 | 4783 | 4784 | 3983 | 2124 | 2468 | 4256 | 4354 | 4301 |
| | Force (Axial) | Right | N | 9040 | 4126 | 4445 | 417 | 3359 | 2757 | 3415 | 4297 | 4826 | 4054 |
| Tibia | Tibia Index | LU | | 1.16 | 0.852 | 0.584 | 0.672 | 0.476 | 0.323 | 0.739 | 0.536 | 0.587 | 0.888 |
| Tibia | Tibia Index | RU | | 1.16 | 0.402 | 0.541 | 1.017 | 0.656 | 0.540 | 0.501 | 0.508 | 0.661 | 0.365 |
| Tibia | Tibia Index | LL | | 1.16 | 0.690 | 0.645 | 0.566 | 0.392 | 0.210 | 0.402 | 0.548 | 0.190 | 0.651 |
| Tibia | Tibia Index | RL | | 1.16 | 0.285 | 0.535 | 0.821 | 0.465 | 0.539 | 0.328 | 0.396 | 0.485 | 0.305 |
| Tibia | Tibia Index | Max | | 1.16 | 0.852 | 0.645 | 1.017 | 0.656 | 0.540 | 0.739 | 0.548 | 0.661 | 0.888 |
| Ankle | [in/e]version | Left | deg | 35 | 42.7 | 45.5 | 101.0 | 78.8 | 31.9 | 90.4 | 81.9 | 94.4 | 57.7 |
| Ankle | [in/e]version | Right | deg | 35 | 41.7 | 61.4 | 16.9 | 52.8 | 36.3 | 84.4 | 37.8 | 76.6 | 68.0 |
| Ankle | [p/d]flexion | Left | deg | 35 | 21.6 | 26.0 | 27.9 | 26.5 | 22.5 | 29.8 | 32.4 | 38.4 | 25.6 |
| Ankle | [p/d]flexion | Right | deg | 35 | 19.9 | 16.5 | 45.9 | 31.2 | 26.5 | 34.2 | 22.2 | 34.6 | 14.5 |
| Ankle | Rotation | Max | deg | 35 | 42.7 | 61.4 | 101.0 | 78.8 | 36.3 | 90.4 | 81.9 | 94.4 | 68.0 |
| Belt | Lap Belt | Max | N | NA | 6213 | 3461 | 9346 | 5629 | 6536 | 8271 | 5108 | 4118 | 4153 |
| | Shoulder Belt | Max | N | NA | 4923 | 4740 | 4479 | 3354 | 4236 | 5531 | 2823 | 3280 | 2889 |